Geothermics 53 (2015) 429–445

Contents lists available at ScienceDirect

Geothermics

journal homepage: www.elsevier.com/locate/geothermics

Potential biogeochemical impacts of heat rejection in the Mullaloo aquifer, Western Australia

G.B. Douglas[a,*], M.G. Trefry[a], J.T. Wylie[a], P.G. Wilkes[b], G.J. Puzon[a], A.H. Kaksonen[a]

[a] CSIRO Land and Water, Private Bag 5, Floreat, WA 6913, Australia
[b] CSIRO Mineral Resources, 26 Dick Perry Avenue, Kensington, WA 6151, Australia

ARTICLE INFO

Article history:
Received 29 May 2012
Accepted 4 August 2014

Keywords:
Heat rejection
Groundwater
Biogeochemical protocol
Geochemistry
Microbiology
Modelling

ABSTRACT

A rapid biogeochemical assessment protocol has been developed to assess the potential effects of returning heated groundwater to the Mullaloo aquifer in Perth, Western Australia. A multi-disciplinary study encompassed geochemical analysis of the aquifer sediment, and microbiological, organic contaminant and major ion surveys of the groundwater. Geochemical modelling indicates few, if any adverse implications of a proposed 10 °C temperature increase. A potential exists for chemical and biological clogging but this will be minimised by a closed loop design to avoid the introduction of atmospheric oxygen. Nevertheless, the need for regular monitoring of scheme performance and environmental impacts remains.

1. Introduction

Efficient operation of high net heat-producing infrastructure common in major industry and in urban centres generally requires the efficient harvesting and disposal of excess heat energy (e.g. Tawney et al., 2005). Typically in industry, heat exchangers are employed to capture excess energy for utilisation elsewhere in plant operations, or alternatively, heat loss is facilitated by direct venting of steam/water vapour to the atmosphere, often via cooling towers. It is possible to avoid this loss of heat and water by utilising the thermal and hydraulic properties of the terrestrial subsurface to store heated waste waters underground for later recycling. This kind of energy and fluid engineering is well developed in the geothermal sector.

Within the geothermal industry, surplus hot water previously abstracted and utilised in power generation or in heat exchange applications is often disposed of by re-injection to local aquifers (Horne, 1982; Panichi, 2004). The re-injection of the surplus hot water provides pressure support to the geothermal resource (to maintain pumping performance) and also conserves water which is increasingly becoming a valued resource in its own right.

Sustainability of geothermal systems is an important factor in the economic and engineering feasibility of geothermal applications. Assessments of sustainability must integrate diverse disciplines, including:

- hydrogeology, hydraulics and reservoir engineering;
- geophysics and geomechanics;
- biogeochemistry (geochemistry and microbiology);
- environmental engineering, hydrology, ecotoxicology and ecosystems science;
- economics, geothermics, engineering and facilities management; and
- together with the interests of stakeholder groups as diverse as community residents, government authorities, regulators, industry, finance and environmental groups.

Sustainability studies have been undertaken over the past few decades to assess the economic feasibility and potential environmental impact of thermal energy in groundwater including potential thermal breakthrough (e.g. Papadopulos and Larson, 1978; Holm, 1986; Perlinger et al., 1987; Brons et al., 1991; Griffioen and Appelo, 1993; Kuhn et al., 2002; Banks, 2009; Brielmann et al., 2009, 2011; Bonte et al., 2010, 2011), impact on pathogens (Winters, 1992), and in particular for seasonal aquifer thermal energy storage and recovery (e.g. Dincer, 2002; Ferguson, 2007; Kim et al., 2010; Li et al., 2011; Yu et al., 2011) and long-term impacts on groundwater temperature (Ferguson and Woodbury, 2006).

Locally, the Perth Basin has become a focus for geothermal exploration with the first land release in 2008 (Ghori, 2008). A

* Corresponding author. Fax: +61 8 9333 6499.
E-mail address: Grant.Douglas@csiro.au (G.B. Douglas).

http://dx.doi.org/10.1016/j.geothermics.2014.08.004
0375-6505/

number of studies have examined the potential for exploitation of energy from geothermal reservoirs, some of which are up to 200 °C (Chopra and Holgate, 2007; Regenauer-Lieb and Horowitz, 2007).

The present study is motivated by the need to explore efficient and sustainable technologies to manage the waste heat budget of the Pawsey Supercomputer Centre, now under construction to support Australia's bid for the Square Kilometre Array (SKA) radiotelescope (iVEC, 2010). The Pawsey Centre will house a petascale supercomputing system with an anticipated heat load of 2.4 Megawatt thermal (MW_{th}). Critically, heat disposal options are constrained by the location of the supercomputer within an existing urban environment in addition to that of the proposed supercomputer research facility. Application of conventional cooling towers to directly cool the computer in-rack cooling system would result in a projected water loss, also potentially sourced from local groundwater, of ca. 28–36.5 ML/annum. An alternative option for cooling the supercomputer is the use of local groundwater abstracted from the underlying Mullaloo aquifer, to be passed through a plate heat exchanger in a closed loop with the heated groundwater and re-injected into the aquifer, resulting in minimal net loss of groundwater. The Mullaloo aquifer has a relatively uniform thermal profile over its thickness at the Pawsey site.

The proposed 2.4 MW_{th} heat rejection load of the Pawsey Supercomputer could be met by elevating Mullaloo water temperature within the heat exchanger by an amount ΔT. The higher ΔT, the lower the flow rate of water required to meet the heat rejection load. It has been calculated that for $\Delta T = 5\,^{\circ}C$, a water supply of 1.51 GL/annum/MW_{th} would be required to cool the supercomputer, equating to about 115 L s^{-1}. For $\Delta T = 10\,^{\circ}C$, the required water supply is reduced to 0.75 GL/annum/MW_{th} and the flow rate is halved to approximately 57.5 L s^{-1}. The return of heated water (which will not be reused) to the aquifer may potentially impact the biogeochemistry of the local formation, and hence affect the performance and sustainability of the heat rejection system.

To further investigate the suitability and long-term environmental sustainability of the local groundwater abstraction/heat exchange/re-injection option, we have developed and applied a rapid biogeochemical assessment protocol for the Mullaloo aquifer. Critically, groundwater-dependent ecosystems such as wetlands and native vegetation are directly linked to and partially dependent on the superficial aquifer situated immediately above the Mullaloo aquifer and thus, an increase in temperature has the potential to influence ecosystem function. Furthermore, the proximity (ca. 200 m downgradient) of residential and other urban land uses to the Pawsey site with an extensive local shallow bore network means that there is a range of simultaneous water demands that must also be supported by any subsurface activity. In this way, the Mullaloo aquifer characterisation case study acts as a useful analogue for geothermal applications and resultant temperature fluctuations in many shallow aquifer systems within urban environments around the world.

The biogeochemical effects of increased temperatures are well known for a range of systems and include changes in the solubility of salts and gases, changes in mineral solubility, and hence, the degree of water–rock interaction, and a potential for enhanced microbial productivity. There is currently, however, little specific knowledge of the biogeochemistry of the Mullaloo aquifer, and in particular, its sensitivity to changes in the prevailing thermal environment. In this study, the major biogeochemical elements of the Mullaloo groundwater/aquifer system, specifically the prevailing groundwater and sediment composition and the microbial population, have been studied using a rapid assessment protocol to discern possible environmental effects, if any, of sustained reinjection of groundwater at higher than ambient temperatures. An additional benefit of the assessment protocol is quick identification of knowledge gaps that subsequent studies can focus on to improve project monitoring and management plans and hence reduce overall geothermal implementation risks.

Key elements of the proposed protocol include thermal, geochemical and microbiological assessment (using depth-dependent sampling), and thermal biogeochemical modelling. Together results of the sampling and subsequent analyses and interpretations may be used as input to environmental impact assessment studies required by regulatory authorities and as a baseline for future monitoring and assessment.

The structure of the paper includes first a brief summary of the known hydrogeology of the Pawsey site and the Mullaloo aquifer. Then the rapid assessment protocol is stepped through by application of its elements to the Mullaloo aquifer in following sections. We proceed now to a summary of the findings of prior hydrogeological characterisation studies (Rockwater, 2011a,b,c) which provide useful context and input for the rapid assessment protocol.

2. Pawsey Centre site characteristics

A description of the site characteristics and hydrogeology outlined below are principally derived from previous studies (Rockwater, 2011a,b,c) and references contained therein. The Australian Resources Research Centre (ARRC) precinct is located on the Swan Coastal Plain, about 4.5 km south-east of Perth in Western Australia (Fig. 1). The land allocated for the Pawsey Centre covers an area of about 2 ha adjacent to the existing ARRC building.

2.1. Local geology

The two uppermost aquifers present at the Pawsey site are the unconfined superficial aquifer and the underlying semi-confined Mullaloo aquifer (Fig. 2). The Mullaloo aquifer occurs within a paleochannel deeply incised into the Kings Park formation (Quilty, 1974). Further detailed descriptions of the aquifers are provided by Davidson (1995) and Davidson and Yu (2006). A brief description of the regional setting for the early Tertiary Mullaloo sandstone member (MSM), the target heat rejection zone, based on Davidson and Yu (2006) and previous work undertaken (Rockwater, 2011a,b), is given below. The superficial and Mullaloo aquifers are separated by a confining unit composed of cemented sand and shale. The Mullaloo aquifer is underlain by confining units in the Kings Park Formation which is principally composed of shale and siltstone. The MSM has been identified within the footprint of the Kings Park Formation but its extent has not been accurately defined. Previous studies undertaken by Davidson (1995) and Davidson and Yu (2006) and data from the drilling programme carried out during August and September 2011 at the ARRC (Rockwater, 2011b), were also assessed for this study. At the site, the MSM unconformably overlies shale of the Kings Park Formation, and unconsolidated Bassendean Sand unconformably overlies the MSM. The revised interpretation is based on comparison between lithological and geophysical data from Mullaloo production bore MPB 01, Mullaloo monitoring bores MB 04a, AM40B, AM40D and local production bores.

2.2. Hydrogeology

2.2.1. Superficial aquifer

The superficial aquifer at the site consists of medium grained leached Bassendean Sand. Aquifer hydraulic conductivity is high, ranging from 10 to 50 m d^{-1} (Davidson and Yu, 2008). The pumping test results from nearby superficial bores, CSIRO 1 and DEC 1, indicate that the superficial aquifer hydraulic conductivity is likely to be greater than 60 md^{-1} at the site. Assuming a saturated thickness of about 30 m as inferred from hydrogeological sections, the aquifer

Fig. 1. Location of Mullaloo formation borehole MB04a in suburban Perth, Western Australia.

transmissivity ($T = K \times$ thickness $= 60 \times 30$) is calculated to be very high, approximately 1800 $m^2\,d^{-1}$ (Rockwater, 2011a).

2.2.2. *Mullaloo aquifer*

At the site, the Mullaloo aquifer consists of medium to very coarse-grained, possibly glauconitic, clay-bearing and occasionally carbonate-bearing sandstone. The MSM can be subdivided into three sub-units: an aquitard composed of an organic-rich, sulphidic, viscous, black clay a few metres in thickness underlain by aquifer units of variable thickness composed of slightly glauconitic, clay-bearing sandstone. The basal unit is coarser-grained with porosities as high as 30% (Rockwater, 2011b). The Mullaloo aquifer is interpreted to be 85–88 m thick at the ARRC (CSIRO 1 bore). Based on the pumping test results (Rockwater, 2011b) estimated aquifer coefficients are: an average transmissivity of about 3675 $m^2\,d^{-1}$, a hydraulic conductivity of approximately 43.5 $m\,d^{-1}$, a storativity of 0.7–0.75 $\times\ 10^{-5}$ (i.e. specific storage of 0.8–0.85 $\times\ 10^{-7}\,m^{-1}$) and an effective porosity of 23–30%. The pumping test results

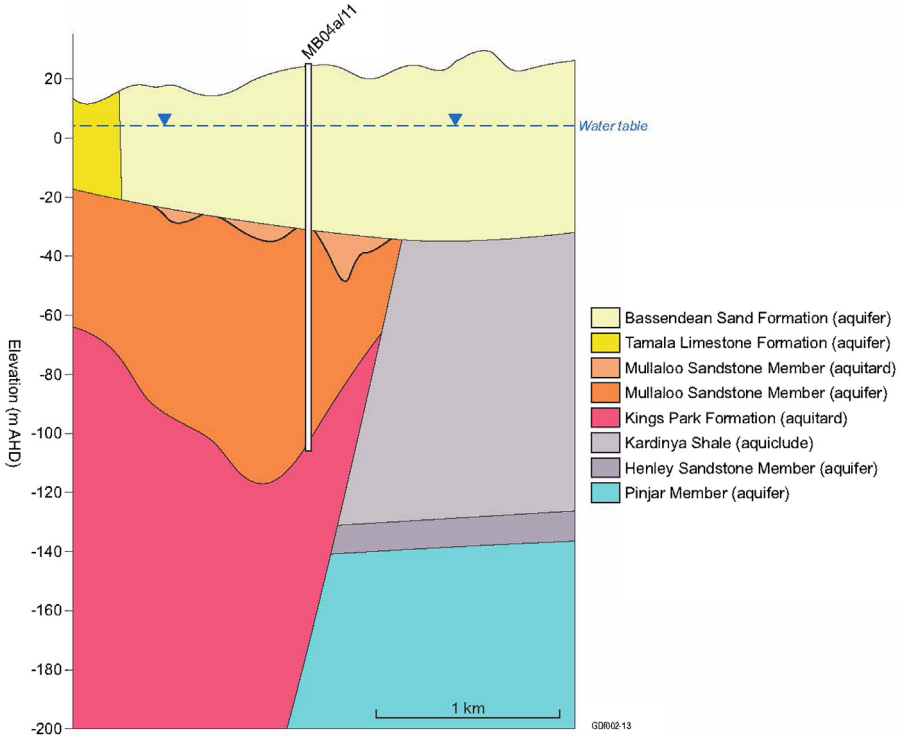

Fig. 2. Local geology of the Mullaloo formation and borehole MB04a.

indicate that the Mullaloo aquifer is semi-confined. The aquitard unit at the top of the MSM, which separates the MSM from the overlying superficial formations is extensive but allows some downward leakage from the superficial aquifer. A constant rate test indicated the average bulk transmissivity of the aquitard to be approximately 2.7 $m^2 d^{-1}$ which may be used in place of a direct measurement of the vertical conductivity of the aquitard. The aquitard transmissivity is thus seen to be approximately three orders of magnitude smaller than the transmissivity of the Mullaloo formation.

The hydraulic conductivity of the Mullaloo aquifer from the recent field investigation (August–September, 2011) is relatively high when compared to the average regional hydraulic conductivity derived from the previous studies (Davidson and Yu, 2006; Rockwater, 2011a). However, it should be considered in the context of a heterogeneous palaeochannel aquifer, where highly transmissive lenticular sandstone beds occur within less permeable strata. Assumptions associated with the standard analytical methods are therefore not always met and the results should be viewed as indicative and suitable for use as starting parameters for a numerical model. The average regional hydraulic conductivity is likely to be lower with the effective mean dominated by areas of low hydraulic conductivity.

2.2.3. Recharge and storage

The superficial aquifer is recharged directly by rainfall infiltration, with groundwater levels strongly influenced by annual and seasonal variations in rainfall. Recharge to the superficial aquifer on the Swan Coastal Plain is also influenced by land use, with values ranging from 20 to 50% of rainfall or more, depending on vegetation type and urban cover. Discharge from the superficial aquifer is predominantly into the Swan-Canning River system with some downward leakage into the Mullaloo aquifer. Additional recharge into the Mullaloo aquifer is likely to occur by lateral flow from the Mirrabooka aquifer to the north of the study area, and from other transmissive intervals to the south and east of the study area. Groundwater from the Mullaloo aquifer is likely to be discharged westward towards the coast into the superficial formations offshore (Davidson and Yu, 2006). Net recharge to the Mullaloo aquifer has not been quantified due to uncertainty in aquifer extent and also in the extent of the overlying aquitard. Based on the drilling and testing investigation in August 2011 (Rockwater, 2011b), the approximate volume of groundwater storage is calculated to be about 1.25×10^8 m^3 assuming an aquifer area of 12.5 km^2, an average thickness of 50 m and a specific yield of 0.2.

2.2.4. Groundwater conditions

Limited studies of local groundwater quality conducted by Rockwater (2011a,b,c) indicate that both the superficial and underlying Mullaloo aquifers are of near neutral pH, low electrical conductivity (EC), and of an Na-Cl type with slightly higher Eh in the superficial aquifer and temperatures typically around 20–21 °C (based on the temperature of water produced at the surface from well fully screened within the Mullaloo formation). Subsequent thermal profiling performed by the Western Australian Geothermal Centre of Excellence (WAGCOE) in November 2011 shows that the water temperature within the Mullaloo formation varied from 20.3 to 20.7 °C over the depth interval 44–132 m below ground surface (Fig. 3). Shallow temperature departures within the superficial aquifer (Bassendean Sand, upper portion of the profile in Fig. 3) are due to seasonal mechanisms, including variation of the land surface temperature (warm in summer and cool in winter) and variation of the water table elevation (high in winter-spring and low in summer-autumn). Together with diurnal solar cycles and intermittent precipitation events which infiltrate cool rainwaters

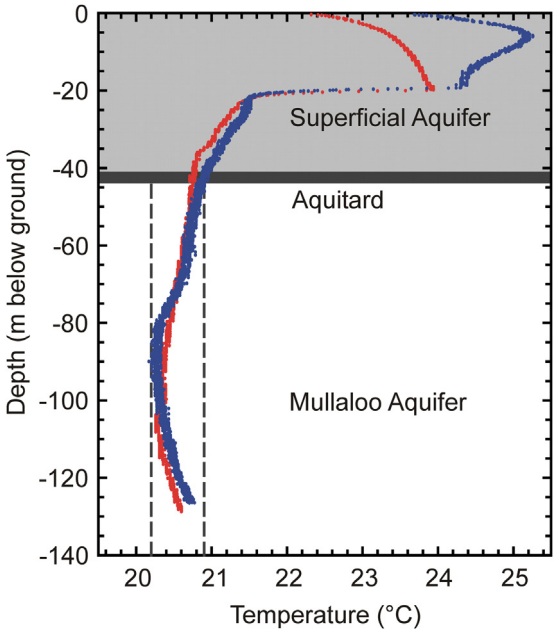

Fig. 3. Thermal profile measured in borehole MB04a. The Mullaloo formation extends between 43 and 130 m depth below ground surface.

through the vadose zone to the water table, these mechanisms often render the near-surface portions of shallow temperature profiles into complex and time-dependent shapes. These climatic perturbations decline with depth. Fig. 2 shows a slight increase of temperature with depth from the ground surface to the water table, then a rapid decline in temperature within the superficial Bassendean Sand unit. Above 30 m below ground surface, the profile will vary significantly with time throughout the annual cycle, but the temperature within the Mullaloo formation is consistent year-round.

2.2.5. Regional flow and thermal breakthrough

Information on the natural head gradient within the Mullaloo aquifer is scarce. The gradient is thought to flow predominantly to the west and estimates of the gradient magnitude are approximately 0.001 m/m with high uncertainty. Assuming hydraulic conductivity of 60 m d^{-1} and a porosity of 30%, this yields an approximate flow velocity of 0.2 m d^{-1}. Thermal breakthrough between extraction and injection wells has been analysed by Gringarten and Sauty (1975). Where the regional flow outweighs the gradient induced by pumping it is possible to avoid thermal breakthrough. The borefield system at the Pawsey Centre site has been designed in order to minimise the potential for thermal breakthrough. Discussion on the engineering design features for mitigating the risk of thermal breakthrough is beyond the scope of this paper.

The heat plume created by injection of warmed water into the Mullaloo will migrate and disperse with regional groundwater flow towards the aquifer discharge boundary. The local head gradient estimates indicate that the discharge boundary is approximately 2.5 km to the west at the Swan-Canning Estuary. Due to the confining shales most of the heat will be contained in the Mullaloo aquifer, with minimal impact on the nearby shallow groundwater users. Discharge rates to the estuary will be slow in comparison to surface water mixing processes, so impacts of any discharging warm water plume on the surface water ecosystem are likely to be negligible.

3. Methods

3.1. Groundwater sampling and analysis

Three sets of groundwater samples were collected in three stages, at sampling depths (below ground surface) of 51, 70 and 90 m (stage 1 average depth 70 m), 99, 105 and 111 m (stage 2 average depth 105 m), and 114, 120 and 126 m (stage 3 average depth 120 m) using an electrically actuated snap sampler system (Snap Sampler, 2011). After deployment, the snap samplers were left in situ for three days to allow for sample flushing and equilibration. For each sampling depth, the sampling apparatus were comprised of five collection containers; 3 × 40 mL glass snap samples for collection of samples for organics analysis, and 2 × 350 mL plastic samples for major and trace ion analysis. Samples obtained from each of the three depths in each stage were aggregated for major and trace ion analysis to comprise a single sample which was then subdivided.

Upon retrieval, the glass snap sampler vials were removed first, snap sampler tabs cut from each end and capped before being labelled and stored on ice in darkness before being transported to National Measurement Institute (NMI) for organics analysis. The plastic snap sampling bottle contents were transferred into separate acid washed plastic bottles. These were pre-rinsed with a small volume of the sample water, and then 500 mL was collected without headspace for analysis of major elements and alkalinity. A 250 mL sub-sample was collected for trace element analysis and acidified with a few drops of concentrated high purity nitric acid. Both of these bottles were stored on ice in darkness and transported to the ChemCentre (Western Australia) for analysis. An additional 40 mL water sample was transferred into autoclaved sterile plastic bottles and stored on ice for flow cytometry and DAPI microbial counting at CSIRO. The remaining sample was retained for analysis of pH, Eh and electrical conductivity with a field kit.

3.2. Major and trace element analysis

The major and trace element water samples were submitted to the ChemCentre within 2 h of collection for major and trace element analysis. All water samples were filtered through 0.2 μm syringe filters prior to sample submission. All analytical methods (e.g. pH, EC nutrient species, alkalinity) were based on APHA Standard Methods for the Examination of Water and Wastewater (2005).

3.3. Organics analysis

Groundwater BTEX (benzene, toluene, ethylbenzene, xylene) and C6-C9 total petroleum hydrocarbons (TPH) were determined using a vapour extraction technique followed by separation on a gas chromatography (GC) column and detected using a HP 6980 GC fitted with a 5973 Mass Selective Detector. Total petroleum hydrocarbons (TPH C10–C36) were extracted with dichloromethane and injected into a non-polar GC (Varian 3800 GC) for separation of individual TPH components and detected with a flame ionisation detector. Dissolved organic carbon (DOC) was measured after filtration through a 0.45 μm filter using a high temperature combustion method (850 °C for Ce or 650 °C for Pt reactor). The DOC was converted to CO_2 and was measured by an infrared detector at 4200 nm. A second injection of the sample acidified with 30% H_3PO_4 was used to correct for inorganic carbon.

3.4. Petrographic analysis

Thin sections of epoxy grain mounts of Mullaloo aquifer sediments samples from 51, 54, 111, and 120 m depth were prepared by CSIRO. Thin sections were examined using a Nikon geological microscope under plane-polarised and cross-polarised light fields and saved as digital images.

3.5. Microbial analysis

3.5.1. Flow cytometry (FCM)

An aliquot of each sample was mixed well, diluted 1:10 with tap water filter sterilised with a 0.8/0.2 μm Acrodisc PF Supor Membrane filter (Pall Life Sciences) and the cells were stained with green fluorescent nucleic acid stain SYTO-9 (Invitrogen Live/Dead Bac Light Bacterial Viability Kit, final concentration 2.7 μM). This binds to the DNA of both live and dead cells after an incubation period of 15 min at room temperature in the dark for FCM. After incubation, samples were further diluted 1:10 in the filter sterilised tap water giving a final dilution of 1:100. As a control, aliquots of each sample were also filtered through a 0.8/0.2 μm filter and thereafter stained as described above for FCM.

All FCM experiments were performed using a Cell Lab Quanta™ SC Beckman Coulter flow cytometer equipped with an air-cooled 15 MW argon ion laser, emitting at a fixed wavelength of 488 nm. Fluorescent filters and detectors were all standard with green fluorescence collected in the FL1 channel (530 ± 30 nm), orange fluorescence collected in the FL2 channel (585 ± 42 nm) and red fluorescence collected in the FL3 channel (>670 nm). All parameters were collected as logarithmic signals (Hoefel et al., 2003). Data were analysed using Cell Lab Quanta® SC MPL Analysis software.

3.5.2. Epifluorescence microscopy

For epifluorescence microscopy, 1 mL of sample was stained with DNA-binding dye 4′,6-diamidino-2-phenylindole, dihydrochloride (DAPI) (100 μg mL^{-1}) for 1 min and the cells were collected onto a 0.2 μm Isopore membrane filter. The filter was then mounted onto a microscope slide with immersion oil and a cover slip and viewed with 100× objective under fluorescence using a Zeiss microscope fitted with an Axio Imager M.1. At least 20 fields of view were counted on the computer screen for each sample.

3.6. Geochemical modelling

Mineral saturation indices (SI) of an average groundwater chemistry from the three samples collected in this study from 20 to 50 °C were calculated using PHREEQC for Windows version 2.18.00 (Post, 2011). Minerals identified in mineralogical (XRD) analysis were used as equilibrium phases.

A pe-pH speciation (Pourbaix) diagram for Fe using an average groundwater chemistry from the three samples collected in this study was calculated using The Geochemists Workbench Release 5.0 (Bethke, 2004).

3.7. Sediment sampling and analysis

Subsamples of aquifer sediments from depths of 51 m, 90 m, 111 m, and 120 m from borehole MB04a were collected from Rockwater who had previously gently washed and sieved the samples to remove remnant drilling mud. The samples were then dried overnight in open trays at 80 °C in a laboratory oven prior to analysis.

3.8. Major and trace element analysis

3.8.1. X-ray fluorescence (XRF) analysis – fusion

Aquifer sediment samples were analysed by X-ray fluorescence (XRF) for major elements (wt% oxides): SiO_2, Al_2O_3, Fe_2O_3, MnO, MgO, CaO, Na_2O, K_2O, TiO_2, P_2O_5, and trace elements (μg/g): Ba, Ce, Cl, Cr, Co, Cu, Ga, La, Ni, Nb, Pb, Rb, S, Sr, V, Y, Zn, and Zr using fused glass discs using the methods of Norrish and Chappell (1977).

Table 1
Summary of mineralogy of Mullaloo aquifer sediment samples from borehole MB04a.

Sample	Quartz	Calcite	Dolomite	K-feldspar	Rutile	Pyrite	Kaolinite	Fe oxide[a]
MB04a 51 m	90.1	8.9	<0.5	<0.5	<0.5	0.1	<0.5	
MB04a 90 m	>99							<1
MB04a 111 m	>99						<0.5	
MB04a 120 m	98.4					1.0	0.6	

[a] Poorly crystalline phase.

One gram of each oven dried sample (105 °C) was accurately weighed with 4 g of 12–22 lithium borate flux. The mixtures were fused for 20 min at 1050 °C in a Pt/Au crucible then poured into a 32 mm Pt/Au mould heated to a similar temperature. The melt was cooled quickly over compressed air and the resulting glass disks were analysed on a Philips PW1480 wavelength dispersive XRF using a dual anode Sc/Mo tube and algorithms developed by CSIRO.

3.8.2. X-ray fluorescence (XRF) analysis – pressed powders

Aquifer sediment samples were also analysed by XRF for major elements (wt% element): Si, Al, Fe, Mn, Mg, Ca, Na, K, Ti, P, S, and trace elements (μg/g): Ag, As, Ba, Bi, Br, Cd, Ce, Co, Cr, Cs, Cu, Ga, Ge, Hf, Hg, I, In, La, Mo, Ni, Nb, Nd, Pb, Pr, Rb, Sb, Se, Sm, Sn, Sr, Ta, Te, Th, Tl, U, V, W, Y, Yb, Zn, Zr using pressed powders.

Four grams of each sample was accurately weighed with 1 g of Licowax binder. The mixtures were shaken vigorously for 30 s using a laboratory test tube shaker and pressed with 10 tonnes pressure with a boric acid backing into pellets and then analysed on a Spectro X-Lab 2000 energy dispersive XRF system using a Pd X-ray tube and 5 secondary excitation targets.

3.9. Mineralogy

Aquifer sediment samples were ground (micronized) for 10 min under ethanol, oven dried at 60 °C and lightly pressed into stainless steel holders for X-ray diffraction (XRD) analysis. Diffraction patterns were recorded with a PANalytical X'Pert Pro microprocessor-controlled diffractometer using Co Kα radiation, automatic divergence slit, graphite post-diffraction monochromator and X'Celerator fast Si strip detector. Data were recorded in 0.05° steps 2Θ with a 0.5 s count time per step, and analysed using HighScore Plus and XPLOT.

A fraction of magnetic minerals within the Mullaloo aquifer sediment sample from 51 m depth was collected using a rare earth super magnet which was then sieved to collect the −200 μm fraction to further concentrate the magnetic mineral fraction. An XRD analysis was then undertaken on this fraction using the methods described above.

4. Results

4.1. Mullaloo aquifer sediment mineralogy

4.1.1. Unfractionated sediment

A summary of quantitative mineralogical analysis of unfractionated Mullaloo sediment samples from 51, 90, 111, and 120 m depth from borehole MB04a is shown in Table 1. Stacked XRD patterns for the four Mullaloo aquifer samples are shown in Fig. 4. The results indicate a predominance of quartz (90 to >99%) at all depths sampled within the Mullaloo aquifer. The greatest mineralogical variability occurs within the uppermost sample at 51 m with carbonates, principally calcite and minor dolomite, K-feldspar, rutile, pyrite and kaolinite also present. Within the deepest sample at 120 m, 1% pyrite and minor kaolinite was also present.

4.1.2. Fractionated magnetic mineral separate

The Mullaloo magnetic mineral separate from 51 m depth (Fig. 5) shows the presence of quartz (suggesting the presence of magnetic inclusions therein), ilmenite, rutile and pseudorutile with minor peaks indicating muscovite and kaolinite. A qualitative XRF scan performed on this sample showed a small Cr peak, and in the absence of a Cr-spinel, indicating possible substitution of Cr for Fe in ilmenite or possibly pseudorutile.

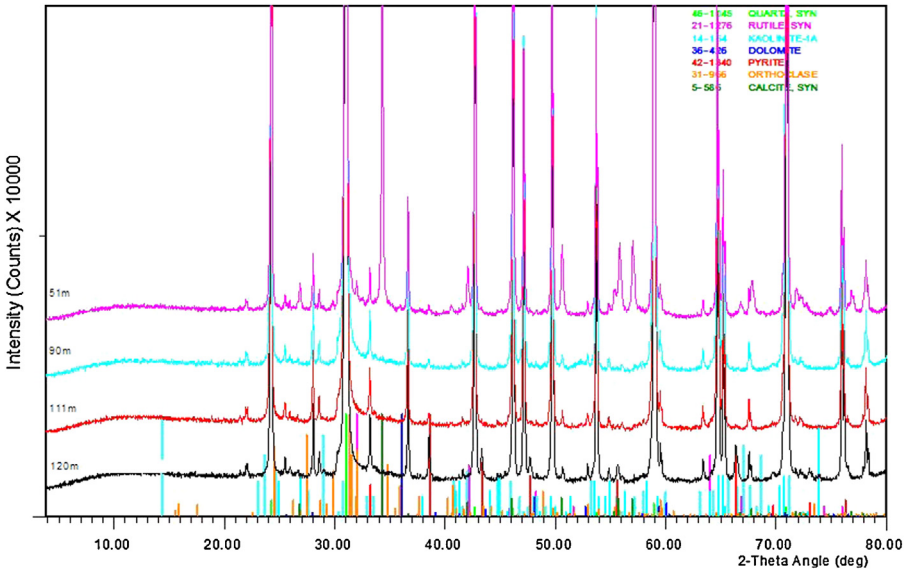

Fig. 4. Stacked X-ray diffraction (XRD) patterns from Mullaloo aquifer sediments from 51, 90, 111, and 120 m depth form borehole MB04a.

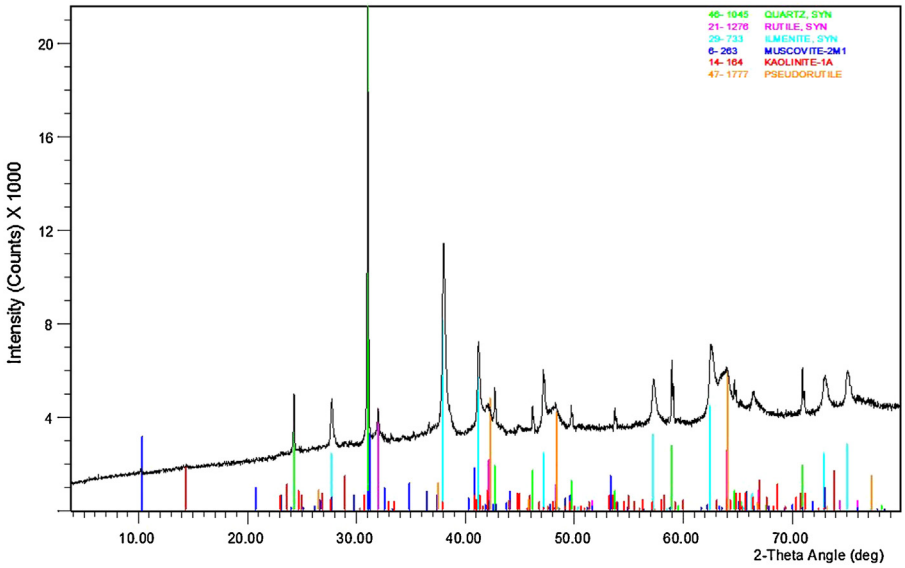

Fig. 5. X-ray diffraction (XRD) pattern of a −200 μm magnetic mineral separate at 51 m depth from borehole MB04a in the Mullaloo aquifer.

4.2. Petrographic analysis

Petrographic analysis of four Mullaloo aquifer sediment samples via optical microscopy revealed a general increase in clast grainsize with depth with the majority of quartz grains, as the predominant mineralogical component, 0.2–1.0 mm along the longest axis in upper samples and 1.0–2.0 mm along longest axis in lower samples and sub- to well-rounded (Fig. 6). Few, if any groundmass minerals are generally present. The Mullaloo aquifer sediments are moderately to well sorted. In general, there is also a more even grainsize distribution with depth, and absence of smaller, often less rounded quartz grains. Monocrystalline quartz grains predominate, however, polycrystalline quartz grains may be present, particularly at depth (see cross-polarised images, 111 m and 120 m depth, Fig. 6).

Minor, often irregular, embayments are often present in larger quartz grains at depth that also frequently host the thickest accumulations of armouring minerals, principally Fe-oxyhydroxides. Minor carbonate grains are evident, particularly at 51 m depth. Occasional opaque to semi-opaque, irregularly shaped organic particles (macerals) are present, particularly in upper samples (Fig. 6). Similarly, minor blocky opaque minerals, typically 0.1 mm in size are present at most depths. Minor rock fragments are also present, particularly in upper samples, however, there is little evidence of discrete clay minerals.

4.3. Mullaloo aquifer sediment geochemistry

Major element geochemical analysis of Mullaloo aquifer sediments from depths 51, 70, 90, 99, 105, 111, 114, 120 and 126 m below ground level reveal a predominantly siliceous composition (ca. 87–99 wt% SiO_2) in accordance with the high quartz concentration identified in mineralogical analyses (Table 2, Fig. 7). Thus, most other major elements (expressed as wt% oxides) are relatively impoverished with only low maximum concentrations of TiO_2 (0.11 wt%), Al_2O_3 (0.84 wt%), Fe_2O_3 (1.24 wt%), MnO (0.015 wt%) Mg O (0.13 wt%), Na_2O (0.09 wt%) and K_2O (0.25 wt%) that are associated with heavy minerals and/or clay minerals, predominantly in the uppermost sediment sample (51 m). The only exception is CaO (5.88 wt%), which is associated with the presence of carbonate minerals, principally calcite as indentified in mineralogical analysis, in the uppermost sample (51 m). Maximum concentrations of both P_2O_5 (0.038 wt%) and SO_3 (0.85 wt%) are low compared to other major element oxides. A compilation of relevant regional and average sediment compositions (from Douglas et al., 2008; Descourvieres et al., 2011; Douglas, unpubl. data) is given in Table 3.

Trace element concentrations are in general low within the Mullaloo aquifer sediments, given the predominance of quartz/SiO_2 (Table 2, Fig. 8). Thus a range of elements including Cd, Co, Cu, Ga, Ge, Mo, Nb, Ni, Pb, Sc, Sm, Th, Tl and U are predominantly below

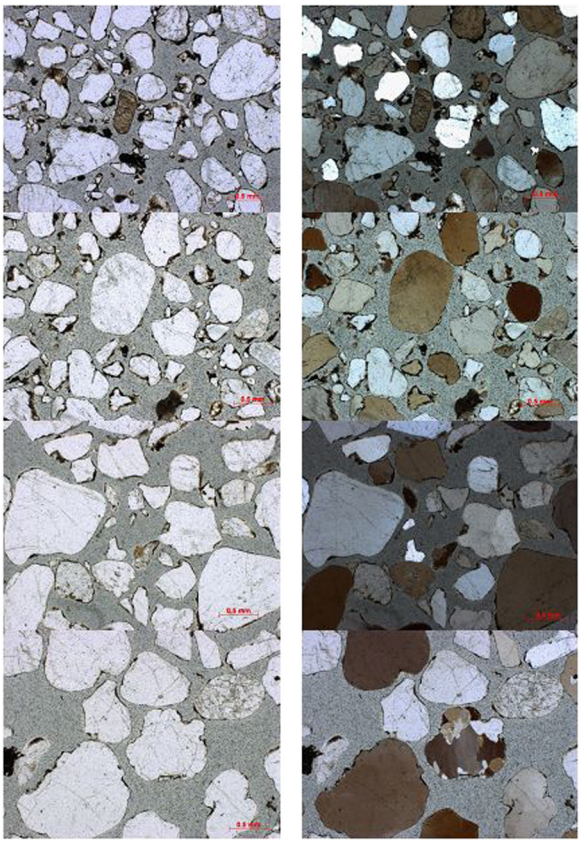

Fig. 6. Thin section photomicrographs of epoxy grain mounts of Mullaloo aquifer sediment at 51, 54, 111, and 120 m. Images in plane-polarized light (left hand side) and corresponding crossed-polarized light (right hand side), respectively.

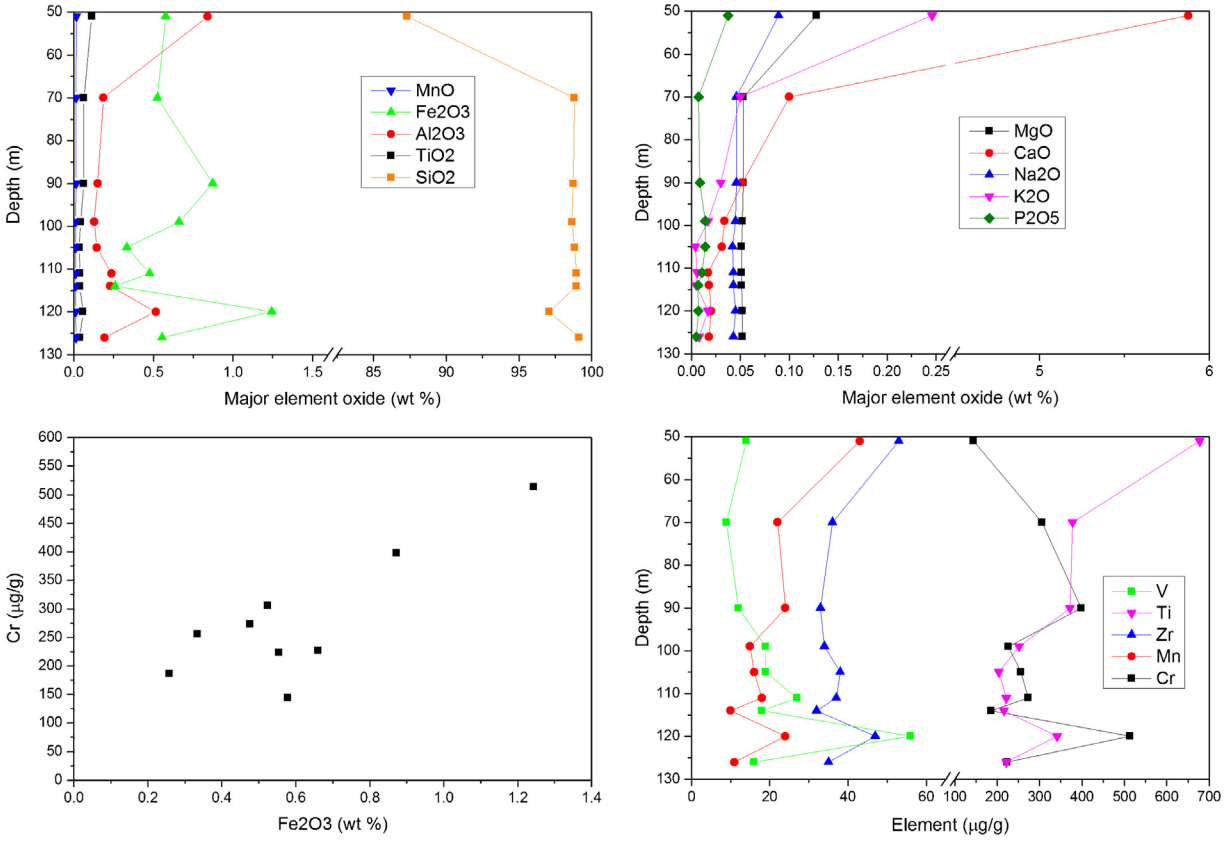

Fig. 7. Variation of major element oxides (wt%) and selected trace elements (µg/g) with depth in the Mullaloo aquifer. Also shown is the relationship between Cr and Fe_2O_3.

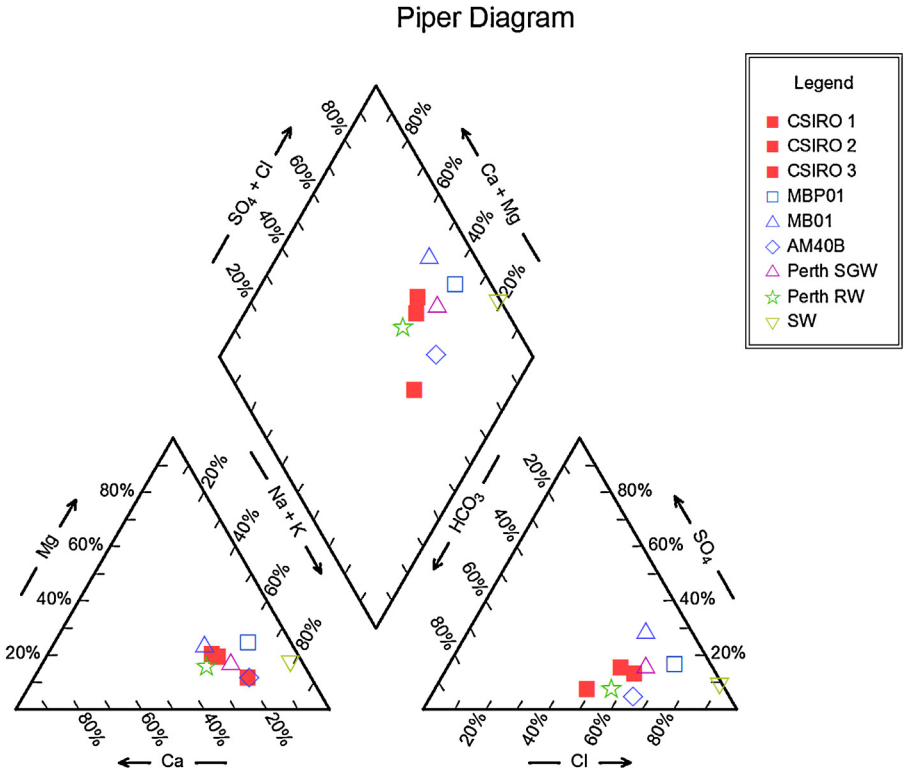

Fig. 8. Piper diagram of Mullaloo aquifer composition collected during the present CSIRO study (1 – 3), by Rockwater (MBP01, Mullaloo aquifer and MB01, superficial aquifer) and by the Western Australian Department of Water (AM40B, Mullaloo aquifer). Also plotted are average Perth superficial groundwater (Perth SGW), Perth rainwater (Perth RW), and seawater (SW) compositions.

Table 2
Major and trace element geochemistry of Mullaloo aquifer sediments.

Sample/element oxide (wt%)	SiO_2	TiO_2	Al_2O_3	Fe_2O_3	MnO	MgO	CaO	Na_2O	K_2O	P_2O_5	SO_3	Sum
MB04a 51 m	87.31	0.11	0.84	0.58	0.015	0.13	5.88	0.09	0.25	0.038	0.17	95.41
MB04a 70 m	98.80	0.06	0.19	0.52	0.013	0.05	0.10	0.05	0.05	0.007	0.05	99.90
MB04a 90 m	98.75	0.06	0.15	0.87	0.013	0.05	0.05	0.05	0.03	0.009	0.01	100.05
MB04a 99 m	98.66	0.04	0.13	0.66	0.012	0.05	0.03	0.05	0.02	0.014	0.03	99.69
MB04a 105 m	98.83	0.03	0.14	0.33	0.011	0.05	0.03	0.04	0.00	0.014	0.02	99.51
MB04a 111 m	98.94	0.04	0.24	0.48	0.011	0.05	0.02	0.04	0.01	0.011	0.10	99.93
MB04a 114 m	98.94	0.04	0.23	0.26	0.011	0.05	0.02	0.04	0.01	0.007	0.07	99.67
MB04a 120 m	97.07	0.06	0.52	1.24	0.011	0.05	0.02	0.05	0.02	0.007	0.85	99.89
MB04a 126 m	99.13	0.04	0.19	0.56	0.012	0.05	0.02	0.04	0.01	0.005	0.43	100.48
Mullaloo average (n = 9)	97.38	0.05	0.29	0.61	0.01	0.06	0.69	0.05	0.04	0.012	0.19	99.39

Sample trace element (μg/g)	As	Ba	Cd	Ce	Co	Cr	Cs	Cu	Ga	Ge	La	Mo	Nb	Nd	Ni	Pb	Rb	Sc	Sm	Sr	Th	Tl	U	V	Y	Zn	Zr
MB04a 51 m	6	74	1.5	6.5	1.5	144	7	5	4	0.5	6	1	3	3.5	0.5	1	9	1.5	4	32	1.5	2	1	14	2	5	53
MB04a 70 m	4	26	1.5	6.5	1.5	306	14	6	0.5	0.5	6	4	3	3.5	0.5	1	2	1.5	4	3	1.5	1	1	9	0.5	1	36
MB04a 90 m	7	16	1.5	6.5	1.5	398	3.5	7	2	1	6	5	3	3.5	0.5	1	2	1.5	4	2	1.5	1	1	12	0.5	3	33
MB04a 99 m	9	17	1.5	6.5	1.5	227	3.5	5	1	0.5	6	2	2	3.5	0.5	1	2	1.5	4	2	1.5	1	1	19	2	5	34
MB04a 105 m	5	24	1.5	37	1.5	256	8	5	0.5	0.5	22	2	2	3.5	0.5	1	1	1.5	4	10	1.5	1	1	19	0.5	5	38
MB04a 111 m	8	14	1.5	18	1.5	273	3.5	5	0.5	0.5	6	2	2	3.5	0.5	1	2	1.5	4	6	1.5	4	1	27	1	10	37
MB04a 114 m	7	17	1.5	6.5	1.5	186	3.5	5	0.5	0.5	6	1	2	3.5	0.5	1	1	1.5	4	2	1.5	4	1	18	0.5	7	32
MB04a 120 m	27	17	1.5	15	1.5	513	10	7	2	1	6	3	3	3.5	3	1	2	3	4	2	1.5	1	1	56	0.5	20	47
MB04a 126 m	26	11	1.5	6.5	1.5	223	3.5	5	0.5	0.5	13	2	3	3.5	0.5	1	1	1.5	4	1	1.5	1	1	16	0.5	6	35
Mullaloo average (n = 9)	11	24	1.5	12	1.5	281	6	6	1.3	0.6	9	2	3	3.5	1	1	2	1.7	4	7	1.5	2	1	21	0.9	7	38

Table 3
Average major and trace element geochemistry of Mullaloo aquifer sediments compared with other local aquifer sediments, Baigup soils, Swan River sediment from Maylands and the Post-Archaean Australian Shale (PAAS).

Sample/element oxide (wt%)	SiO_2	TiO_2	Al_2O_3	Fe_2O_3	MnO	MgO	CaO	Na_2O	K_2O	P_2O_5	SO_3	Sum
Mullaloo average (n = 9)	97.38	0.05	0.29	0.61	0.01	0.06	0.69	0.05	0.04	0.012	0.19	99.39
Bassendean Sand (*n* = 32)	98.17	0.08	0.14	0.41	0.002	0.07	0.06	0.00	0.08	0.003	0.02	98.89
Osborne Formation (*n* = 9)	76.47	0.48	10.39	3.78	0.026	0.45	0.28	0.29	4.61	0.041	0.52	97.34
Leederville Formation (*n* = 175)	77.08	0.54	10.09	2.78	0.020	0.36	0.23	0.34	4.30	0.056	0.46	96.24
South Perth Shale (*n* = 18)	58.38	0.91	17.60	5.29	0.024	1.00	0.77	0.50	3.42	0.224	0.70	88.83
Baigup sub/surface soil (*n* = 140)	63.84	0.46	8.46	4.79	0.019	0.49	1.95	1.25	0.75	0.296	0.40	82.71
Swan River Sediment (Maylands)	66.68	0.51	6.02	3.29	0.026	0.60	1.40	2.18	1.01	0.109	2.06	83.89
Post-Archaean Australian Shale	62.80	1.00	18.90	7.22	2.200	1.30	1.20	3.70	0.16	0.110	n/a	98.59

Sample trace element (μg/g)	As	Ba	Cd	Ce	Co	Cr	Cs	Cu	Ga	Ge	La	Mo	Nb	Nd	Ni	Pb	Rb	Sc	Sm	Sr	Th	Tl	U	V	Y	Zn	Zr
Mullaloo average (n = 9)	11	24	1.5	12	1.5	281	6	6	1.3	0.6	9	2	3	3.5	1	1	2	1.7	4	7	1.5	2	1	21	0.9	7	38
Bassendean Sand (*n* = 32)	1	23	1.5	40	1.5	287	4	3	1	0.5	32	16	9	3.5	16	4	3	1	4	8	8	3	1	9	6	3	71
Osborne Formation (*n* = 9)	4	552	3	52	35	38	7	8	9	2	23	1	7	18	14	15	90	6	6	83	15	10	4	41	10	24	156
Leederville Formation (*n* = 175)	4	546	2	67	41	40	7	8	11	1	35	1	8	24	14	18	102	7	6	69	17	6	4	51	14	37	209
South Perth Shale (*n* = 18)	17	458	3	109	18	93	10	22	23	3	55	1	16	46	40	22	105	12	8	183	32	11	8	87	25	87	273
Baigup sub/surface soil (*n* = 140)	11	178	1.5	46	8	129	6	32	10	2	25	6	9	18	15	62	57	7	5	81	17	11	7	62	12	106	153
Swan River Sediment (Maylands)	n/a	203	n/a	43	7	129	n/a	39	9	n/a	19	n/a	6	n/a	16	76	28	n/a	n/a	88	n/a	n/a	n/a	43	15	475	329
Post-Archaean Australian Shale	n/a	650	n/a	80	23	110	15	50	20	n/a	38	1	19	n/a	55	20	160	n/a	n/a	200	14	n/a	3	150	27	85	210

n/a = not analysed.

Table 4
Compilation of water quality parameters, major, trace element and nutrient concentrations for Mullaloo aquifer (MBP 01) and superficial aquifer (MB 01) samples. All units mg L^{-1} except Eh (mV), EC (μS/cm) and pH.

Sample data							
Bore	MBP 01	MBP 01	MBP 01	MBP 01	MB 01	AM40B	
Sampled	15/12/2011	12/12/2011	8/12/2011	23/09/2011	23/09/2011	1989	ANZECC WQ
Sampled by	CSIRO	CSIRO	CSIRO	Rockwater	Rockwater	WA DoW	
Ave depth (m)	70	105	120	nd	nd	nd	–
In-field water quality parameters							
Field pH	6.58	6.99	6.82	nd	nd	nd	6.5–8.5
Field Eh	392	275	192	nd	nd	nd	
EC μS/cm	no data	441	604	430	512	489	
Major ions							
Na	58.5	55.3	103	51	46	64	n/a
K	4.1	3.9	6.3	3	4	7	
Ca	24.6	25.8	27.1	10	24	17	
Mg	11.2	11.7	9.5	11	12	6	
Cl	92	115	109	85	78	97	250
HCO_3	82	83	167	23	34	78	
SO_4	34.1	33.5	22.2	26	52	9	500
TDS	300	300	380	318	380	nd	n/a
Trace elements							
Ag	<0.0001	<0.0001	<0.0001	nd	nd	nd	0.1
Al	0.094	0.39	0.049	nd	nd	nd	c
As	<0.001	0.003	0.004	nd	nd	nd	0.01
B	0.03	0.04	0.03	nd	nd	nd	4
Ba	0.089	0.081	0.021	nd	nd	nd	2
Cd	<0.0001	<0.0001	<0.0001	nd	nd	nd	0.002
Co	<0.005	<0.005	<0.005	nd	nd	nd	
Cr	0.023	0.027	0.003	nd	nd	nd	0.05
Cu	0.005	0.018	<0.002	nd	nd	nd	2
Fe	0.96	2.7	1.4	0.1	15	1.7	c
Ga	0.0001	0.0003	<0.0001	nd	nd	nd	
Hg	<0.0001	<0.0001	<0.0001	nd	nd	nd	0.001
La	<0.005	<0.005	<0.005	nd	nd	nd	
Mn	0.02	0.19	0.37	nd	nd	nd	0.50
Mo	<0.001	0.002	0.01	nd	nd	nd	0.05
Ni	0.005	0.01	0.009	nd	nd	nd	0.02
Pb	0.0012	0.0048	0.0011	nd	nd	nd	0.01
Se	<0.001	<0.001	<0.001	nd	nd	nd	0.01
Si	9.7	9.8	8.1	12.1	6	16	
Sr	0.054	0.098	0.15	nd	nd	nd	
Th	<0.0001	0.0003	0.0002	nd	nd	nd	
Ti	0.004	0.017	0.004	nd	nd	nd	
U	0.0002	0.0006	0.0002	nd	nd	nd	0.017
V	<0.005	0.006	<0.005	nd	nd	nd	
Zn	<0.005	0.016	0.021	nd	nd	nd	c
Nutrients							
NO_3	12	11	2.9	17.1	26.1	<4	50
NH_3	<0.01	<0.01	<0.01	nd	nd	nd	c
P	0.1	<0.1	1.5	nd	nd	nd	

c – insufficient information to set ANZECC Water Quality guideline, nd – not determined.

or near analytical detection limits for most, if not all, aquifer sediment samples. The highest concentrations of Ba (74 μg/g), and Sr (32 μg/g) are both associated with clay and/or carbonates in the uppermost two sediment samples. Noteworthy, however, are consistently elevated concentrations of Cr (144–513 μg/g) and other trace elements including V (9–56 μg/g) and Zr (32–53 μg/g).

4.4. Mullaloo aquifer water quality

Mullaloo aquifer groundwater chemistry is presented in Table 4 with major ion chemistry for CSIRO samples collected in this study and previous Rockwater and DoW samples plotted in a Piper diagram (Fig. 8). Mullaloo groundwater pH collected in the present study is generally neutral to slightly acidic, however previous Rockwater samples were moderately alkaline (Rockwater, 2011a,b,c). The aquifer waters are predominantly of a Na-Cl type with major cations dominated by Na with lower concentrations of Ca and Mg. Major anions are dominated by Cl with lower concentrations of HCO_3^- and SO_4^{2-}. The aquifer waters are of low ionic strength with TDS < 400 mg L^{-1} (Table 4). These results are similar to that obtained by both Rockwater in 2011 and the Western Australian Department of Water in 1989.

Trace element concentrations are generally low, and depending on the sample, 6–11 of the 25 analytes were below detection limits (Table 4). No trace elements exceed the ANZECC Water Quality Guidelines (ANZECC, 2000). Nutrient concentrations were elevated, particularly for nitrate (2.9–12 mg L^{-1}). Filterable P in one sample from 120 m depth was also elevated (1.5 mg L^{-1}). The nutrient concentrations are sufficient to support microbial growth.

4.5. Organic contaminants and dissolved organic carbon (DOC)

An analysis of the three groundwater samples collected in this present study indicate that all classes of organic contaminants including BTEX and TPH are below detection limits (Table 5). Dissolved organic carbon, expressed as non-purgeable organic carbon showed considerable variability of between 10 and 34 mg L^{-1} for replicate samples from the deepest sample from 114, 120 and

Table 5
Summary of organic contaminant (BTEX, TPH, $\mu g\,L^{-1}$) and dissolved organic carbon ($mg\,L^{-1}$) concentrations for the Mullaloo aquifer.

Class	Sampled Depth	15-12-11 68, 89 m		12-12-11 97, 108 m		08-12-11 114, 120, 126 m		
BTEX	Benzene	<1.0	<1.0	<1.0	nd	nd	<1.0	<1.0
	Toluene	<1.0	<1.0	<1.0	nd	nd	<1.0	<1.0
	Ethylbenzene	<1.0	<1.0	<1.0	nd	nd	<1.0	<1.0
	Xylene	<2.0	<2.0	<2.0	nd	nd	<2.0	<2.0
	Total BTEX	<5.0	<5.0	<5.0	nd	nd	<5.0	<5.0
Total petroleum hydrocarbons	TPH C6–C9	<25	<25	<25			<25	<25
	TPH C10–C14	<75	<25	<25	<25	<25	<25	<25
	TPH C15–C28	<300	<100	<100	<100	<100	<100	<100
	TPH C29–C36	<300	<100	<100	<100	<100	<100	<100
	Total TPH	<700	<250	<250	<250	<250	<250	<250
Dissolved organic C	NPOC[a]	10	34	21	12	<1	1	<1

[a] Non-purgable organic carbon.

126 m. An intermediate sample from 97 m and 108 m also varied from <1 to 12 $mg\,L^{-1}$.

4.6. Microbial biomass

4.6.1. Flow cytometry

The cell counts obtained by FCM for the deep and intermediate samples were lower than the background values obtained for the filtered control samples (data not shown) indicating that the samples contained large amounts of particulate matter that binds the dye, has a size of <0.2 μm and prevents the reliable quantification of microbial cells by FCM. Only the shallow sample gave a cell count 3×10^5 cells mL^{-1} that was above the background value (2×10^5 cells mL^{-1}) of that sample. Since the results from the FCM were inconclusive for the deep and intermediate samples, the samples were also analysed by epifluorescence microscopy for total cell counts.

4.6.2. Epifluorescence microscopy

The cell counts obtained by epifluorescence microscopy for the aquifer samples were 1.4×10^5–5.2×10^5 cells mL^{-1} (Table 6). The cell counts were highest in the deepest sample and lowest in the shallowest sample. The cell counts were in the same range as observed by epifluorescence microscopy for the groundwater in the deep geothermal aquifer of the Great Artesian Basin (GAB), in Australia (10^5–10^6 cells mL^{-1}) (Kimura et al., 2005) and the deep coal seam groundwaters of northern Japan (3.08×10^5 cells mL^{-1}–9.88×10^5 cells mL^{-1}) (Shimizu et al., 2007). Cell counts reported for groundwaters in Virginia have been in the range of 4×10^4–1.2×10^5 cells mL^{-1} (King and Parker, 1988) and those in the groundwaters of ultraoligotrophic alpine springs in the range of 10^4–10^5 cells mL^{-1} (Farnleitner et al., 2005; Wilhartitz et al., 2007). Examples of epifluorescence microscope images of DAPI stained cells from the deep aquifer sample are shown in Fig. 9.

Table 6
Cell counts in the aquifer samples as determined by epifluorescence microscopy of DAPI-stained cells.

Sample	Cells mL^{-1} (ave ± std)
Sample A – deep sample, collected 8/12/11	$5.2 \times 10^5 \pm 2.2 \times 10^5$
Sample B – intermediate sample, collected 12/12/11	$4.4 \times 10^5 \pm 1.9 \times 10^5$
Sample C – shallow sample, collected 15/12/11	$1.4 \times 10^5 \pm 0.9 \times 10^5$

5. Discussion

5.1. Stratigraphic variation

The limited down hole major and trace element and mineralogical variation (Fig. 7) reflects the uniformity of the stratigraphy within the sampled horizons of the Mullaloo aquifer sediments. It is only within the uppermost two horizons that the presence of calcite and minor dolomite increases the CaO concentration and a clay presence that increases the Al_2O_3 and Fe_2O_3, and to a lesser extent MgO, Na_2O and K_2O concentrations. These major element enrichments result in a dilution of quartz abundance, and hence, SiO_2. Similar major element concentration variations also occur due to mineralogical changes, albeit to a lesser extent, further downhole at 120 m, notably due to the presence of minor pyrite contributions (Table 1, Fig. 4). It is noteworthy that no glauconite was identified in the Mullaloo aquifer samples despite it being noted in a previous study (Davidson, 1995).

Trace element concentrations also occur within the Mullaloo aquifer with a remarkably consistent pattern of stratigraphic (down hole) variation for V, Ti, Zr, Mn and Cr (Fig. 7). In the absence of the uppermost carbonate and most clay-rich sample, a similar stratigraphic relationship is present between Cr and Fe ($r^2 = 0.82$), Ti ($r^2 = 0.54$), Zr ($r^2 = 0.55$) and V ($r^2 = 0.43$). This attests to a general relationship between these elements and the intermittent presence of a heavy mineral fraction as identified during heavy mineral separation, notably the likely presence of Cr-bearing ilmenite, and although not identified, possibly chromite, and other heavy minerals such as ilmenite ($FeTiO_3$) and zircon ($ZrSiO_4$). The latter two

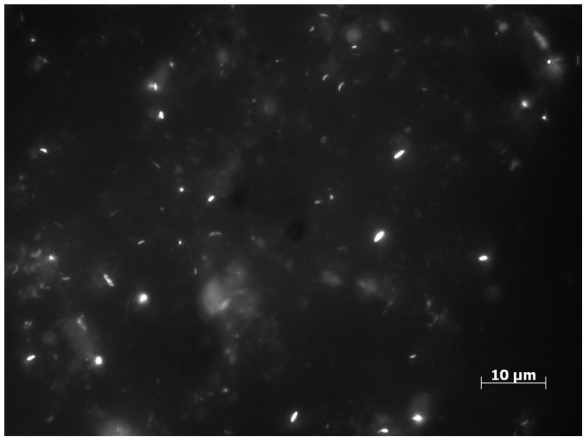

Fig. 9. Epifluorescence microscope image of DAPI-stained aquifer cells from the deep sampling point.

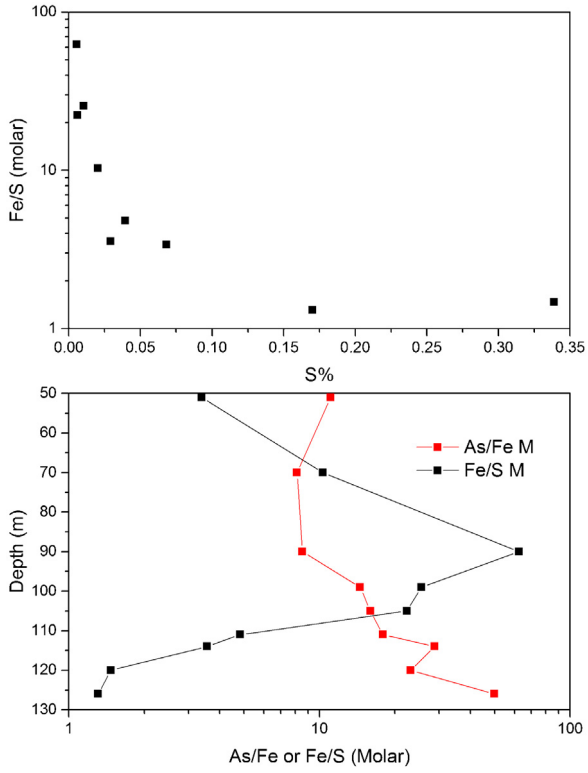

Fig. 10. Geochemical relationships between Fe/S (molar) and S (wt%), depth and As/Fe (molar) and Fe/S (molar).

minerals in particular are known to be common in sands of the Swan Coastal Plain (Gozzard, 2007). Interestingly, the abundance of quartz within the magnetic mineral separates suggests that many of the magnetic minerals are present as inclusions within discrete quartz grains.

Extensive, long-term weathering within the Yilgarn Craton, particularly since the Tertiary, has resulted in the concentration of a range of heavy minerals derived predominantly from mafic/ultramafic lithologies (Anand and Paine, 2002; Cornelius et al., 2008). The heavy minerals then accumulated in sandy sediments of the Swan Coastal Plain (Bastian, 1996; Collins and Baxter, 1984). Heavy minerals such as chromite, magnetite and ilmenite, sometimes present as intergrowths (Groves et al., 1977) have long been recognised as abundant in the Western Australian regolith, and in particular mafic/ultramafic regions of the Yilgarn (Simpson, 1912), while chromium-bearing ilmenites in beach sand deposits in south western, Western Australia have also been observed (O'Shaughnessy, 1973).

Within the Mullaloo aquifer sediments, intermittently enriched Fe in the absence of a significant clay component, and a corresponding enrichment of S indicate the possible presence of pyrite, a common accessory mineral in both superficial (e.g. Bassendean Sand, Yesertener, 2010) and deep (Leederville Formation, Descourvieres et al., 2011) aquifer sediments of the Swan Coastal Plain. The specific presence of pyrite within the deeper portion of the Mullaloo aquifer has also been confirmed by XRD analysis (Table 1). An analysis of the variation of the Fe/S molar ratios with S (wt%) indicates that as the latter increases, the Fe/S molar ratio approaches unity in accordance with the presence of pyrite (Fig. 10). In situ down hole measurements of Eh within borehole MB04a indicate increasingly reducing conditions with depth (Rockwater, 2011a,b,c), again consistent with the presence of pyrite.

The presence of significant pyrite at 120 m depth in the Mullaloo aquifer also corresponds to an increase in As concentrations (Fig. 10). The presence of As-bearing pyrite is common across the Swan Coastal Plain (e.g. Appleyard et al., 2006; Yesertener, 2010), particularly within the superficial aquifer dominated by the Bassendean Sands.

A compilation of Mullaloo aquifer sediments and other regional aquifer sediments, Baigup soils, Swan River sediment from Maylands and the Post-Archaean Australian Shale (PAAS) is given in Table 3. In terms of major, and to a lesser extent, trace element geochemistry, the average Mullaloo aquifer sediment most closely resembles the Bassendean Sand which forms the superficial aquifer at borehole MB04a. Given the mutually high average SiO_2 concentrations, the majority of other elements are impoverished, but for minor CaO and Al_2O_3 enrichment in the average Mullaloo composition due to carbonate and clay enrichment in the uppermost samples. Similarly, most trace elements, including average Cr concentrations, are similar between the Mullaloo aquifer sediments and those of the Bassendean Sand.

By comparison to average Mullaloo aquifer sediments, regional aquifer sediments from the Osborne and Leederville Formations and South Perth Shale, Baigup soils and Swan River sediment encompass a range of major and trace element concentrations that, due to their relatively low SiO_2 concentrations are also substantially enriched (Table 3). In particular these regional aquifer and riverine soils and sediments are more clay-rich, and hence, also enriched often by one- to two-orders of magnitude in both alkali and alkaline earth element oxides/elements such as CaO, MgO, Na_2O, K_2O, Ba, Rb, Sr, in addition to transition metals (Cd, Cu, Ni, Pb, V, Zn) rare earth elements (e.g. La, Ce and Nd), and actinides (Th, U).

Comparison to the Post-Archaean Australian Shale, an estimate of average crustal abundances (Taylor and McLennan, 1985), also suggests Cr enrichment in the Mullaloo aquifer sediments. In addition, the average Mullaloo aquifer sediments are, by virtue of SiO_2 (quartz) enrichment, with its inherent purity, comparatively impoverished for a range of major and trace elements.

5.2. *Mullaloo aquifer groundwater composition*

The major composition of the Mullaloo aquifer groundwater is consistent with derivation from a seawater-Perth rainwater signature (Fig. 8) with minor modification due to water–rock interaction (e.g. carbonate or clay mineral equilibration) as evidenced by variable concentrations of bicarbonate and silica respectively. The Mullaloo aquifer major ion composition is also similar to that of average Perth shallow groundwater (Perth SGW – $n = 103$, after Yesertener, 2010) and that of the superficial aquifer.

Speciation modelling of Fe in the Mullaloo aquifer samples collected in this study is in general agreement with results of mineral stability modelling (as saturation indices) confirming that the majority of Fe is present as Fe-oxyhydroxide minerals (Table 1, Figs. 11 and 12). Groundwater samples previously collected by Rockwater also suggest the possible presence of siderite in more alkaline samples. While pyrite formation is not immediately suggested on the basis of recent Mullaloo aquifer groundwater sampling and Eh–pH monitoring, only a small decline in Eh/pe is nonetheless required to produce conditions conducive to pyritisation, particularly in the presence of sulfate-reducing bacteria known to occur in Swan Coastal Plain sediments (e.g. Robertson et al., 2000, 2001).

Trace element concentrations are often low and are consistent with the predominantly circum-neutral pH and the presence of abundant Fe-oxyhydroxides as coatings on the majority of quartz grains which would be likely to act as sinks for metals. Nutrient concentrations are within ranges commonly encountered in Perth

Table 7
Recommended values for water quality parameters and observed range in Mullaloo aquifer.

Concept		Parameter	Limitations	Range in Mullaloo aquifer
Biological clogging	Deep systems	pH	>7.2 (iron bacteria)	6.58–6.99
		DOC	<2 mg L^{-1}	<1–34 mg L^{-1}
		Eh	>10 mV	192–392
	Surface systems	TOC	TOC < 10 mg L^{-1}	<1–34 mg L^{-1} (DOC)
Chemical clogging		[Fe^{2+}]	<11.2 mg L^{-1}	0.1–15 mg L^{-1}
		pH	<7.5	6.58–6.99
		TDS	<150 mg L^{-1}	300–380
		[Cl^-]	<500 mg L^{-1}	78–250

Source: Adapted from Pérez-Paricio (2000).

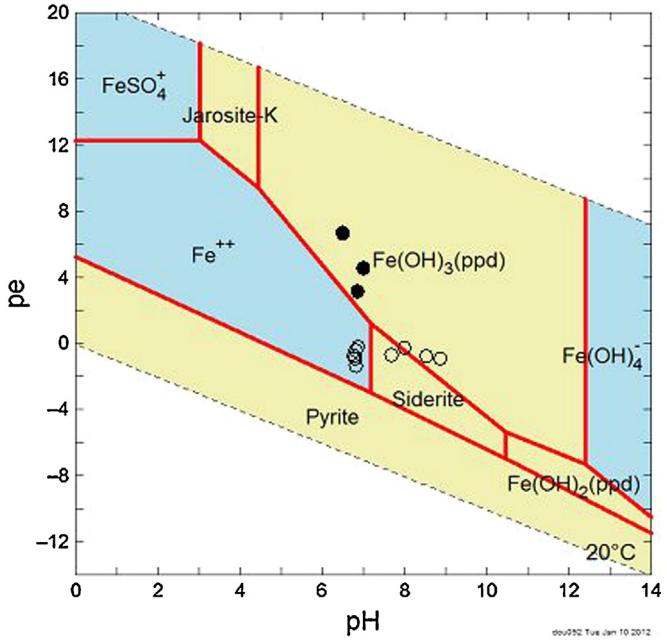

Fig. 11. Pourbaix (pe-pH) diagram of Fe-S-C-O-H system at 20 °C and 1 atmosphere for Mullaloo aquifer groundwater from borehole MB04a. Activities of the major ions are: $Fe^{3+} \times 10^{-5}$, $SO_4^{2-} \times 10^{-4}$, $Cl \times 10^{-3}$, $HCO_3^- \times 10^{-3}$ M based on mean composition of Mullaloo groundwater. Solid mineral fields are in yellow and solutes in blue. The three groundwater samples collected in this study and an approximate pe-pH field derived from CSIRO (solid circles) and Rockwater data (open circles) are also plotted.

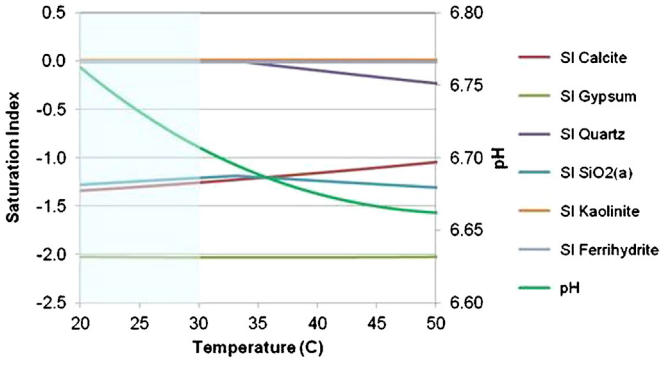

Fig. 12. Saturation indices of Mullaloo aquifer minerals and groundwater pH as a function of temperature from 20 to 50 °C. An average groundwater composition from the three CSIRO samples was used in the model. The forecast range of temperature increase in the Mullaloo aquifer due to the return of heated groundwater (ΔT = 10 °C) is shaded.

superficial aquifers (e.g. Bennett et al., 2007; Yesertener, 2010; Sarukkalige, 2011).

5.3. Microbial substrate and nutrient concentrations

A set of threshold values for biological and chemical clogging are shown in Tables 7 and 8 shows guidelines for clogging and redevelopment of aquifers (adapted from Pérez-Paricio, 2000). Apart from the deepest aquifer samples obtained from 114 to 126 m of the Mullaloo aquifer, DOC concentrations were above the threshold value for bioclogging in deep systems (<2 mg L^{-1}) (Table 7). The TDS was above the threshold limit for chemical clogging in all samples. Ferrous iron concentrations were below the threshold in most samples, except for one sample obtained by Rockwater (2011c). According to the TOC-based guidelines presented in Table 8 and the observed DOC results for Mullaloo Aquifer, the water quality in the deepest samples indicate a slight tendency for bioclogging, where as the shallowest samples indicate a notable or strong tendency for bioclogging. However, it is to be noted that the transformation of natural organic matter (NOM) and microbial growth during artificial groundwater recharge is dependent on a number of site specific and operational factors as shown in Fig. 13. Guidelines for the redevelopment of aquifers to prevent clogging are given in Table 8.

5.4. Effect of increased temperature on Mullaloo aquifer geochemistry

Geochemical modelling of the groundwater geochemistry indicates that subtle changes in mineral solubility occur as a function of increasing temperature (Fig. 12). Similarly, groundwater pH only marginally declines from ca. 6.75 to 6.65 over the 30 °C temperature increment modelled in this study. This potential pH change is likely to be well within the natural pH variation of fluids within the greater Mullaloo aquifer. Lower temperature changes are predicted to result in even smaller perturbations to the solubilities of dominant mineral phases and the pH (see the shaded zone in Fig. 12 corresponding to a ΔT of 10 °C).

Mineral dissolution rates may be both enhanced and suppressed with changes in ambient temperature (e.g. Aargard and Helgeson, 1982). Within the Mullaloo aquifer, modelled mineral solubilities only display small changes in solubility as a function of temperature. In particular, quartz, which is at equilibrium with the prevailing groundwater, and amorphous silica, albeit the latter already undersaturated, display a small increase in predicted solubility (as saturation index), particularly at temperatures greater than ca. 35 °C (Fig. 12). Given that predicted temperatures of returned water are unlikely to exceed 30 °C, it is unlikely that any discernible change would occur in terms of quartz dissolution or concomitant groundwater composition. Furthermore, the modelling conducted here only considers thermodynamics in terms of the saturation index, and does not include a kinetic term. Many studies conducted on quartz dissolution, however, indicate

Table 8
Guidelines for clogging and redevelopment based on TOC.

	Clogging	Recharge water	Redevelopment
Surface systems	Slight	TOC < 10 mg L^{-1}	Natural drying and cracking Once a year mechanical
	Notable	TOC = 10–25 mg L^{-1}	Frequent drying and cracking Twice a year mechanical
	Strong	TOC > 25 mg L^{-1}	Prefiltration recommended
Deep systems	Slight	TOC < 10 mg L^{-1}	Frequent pumping Once a month surging/jetting
	Notable	TOC = 10–25 mg L^{-1}	Pumping once a day Once a week surging/jetting
	Strong	TOC > 25 mg L^{-1}	Daily pumping Adapted protocol

Source: Adapted from Pérez-Paricio (2000).

that rates of crystalline quartz dissolution are exceedingly slow (ca. 10^{-16} mol cm^{-2} s^{-1}, Brady and Walther, 1990), particularly in freshwaters, with minimum dissolution rates at solution pH of ca. 4–6, similar to that of the prevailing Mullaloo aquifer groundwater. Similarly a temperature increase from ca. 20 to 30 °C as envisaged in the Mullaloo aquifer will be unlikely to significantly enhance dissolution rates of ambient dissolved Si concentrations. Similarly, mixing with incumbent groundwater upon return to the Mullaloo aquifer is likely to quickly decrease the temperature such that changes to solute composition from mineral dissolution, which is already small, will be negligible on a more widespread basis. A further barrier to any potential quartz dissolution is the armouring of part of, or entire quartz grains, by Fe-oxyhydroxides. This armouring is likely to provide an additional physico-chemical barrier to dissolution.

In contrast, calcite, present as a minor mineral, particularly within the upper Mullaloo aquifer displays a small decrease in solubility similar to that observed in other studies (e.g. Kuhn et al., 2002). Nonetheless, calcite remains over an order of magnitude undersaturated and thus, the groundwater composition will remain essentially unaffected. Gypsum remains strongly undersaturated over the entire temperature range.

Both ferrihydrite (as a proxy for a range of Fe-hydroxides/oxyhydroxides) and kaolinite (partially obscured) both remain in equilibrium (SI = 0) with the prevailing groundwater over the entire temperature range. Thus, it is unlikely that trace elements associated with these minerals will be mobilised during any increase in groundwater temperature.

5.5. Development of an operational protocol for the Pawsey Centre groundwater cooling system

Based on the characterisation of the aquifer sediments, groundwater chemistry and microbiology, a monitoring protocol has been developed for the operation of the Pawsey Centre Groundwater Cooling system. This protocol has been designed to ensure the safe and efficient operation of the groundwater cooling system by comparing baseline aquifer biogeochemistry with indicators measured throughout the operational lifetime of the heat rejection system.

Monitoring of a range of physical, geochemical and microbiological parameters is critical to ensure that changes in groundwater do not result in compositional changes detrimental to ecosystem function or system operation. For instance, increased oxygen ingress may potentially result in increased acidity and trace element mobilisation due to sulfide oxidation or alternatively, Fe precipitation and scaling. Similarly, changes in oxygen status, whether increased or decreased may influence nutrient speciation such as P release from reductive dissolution of Fe-oxyhydroxides, nutrient transformation (e.g. microbial oxidation of NH_3 to NO_3^-) or rates of mineralisation, and possible changes in microbial biomass or composition.

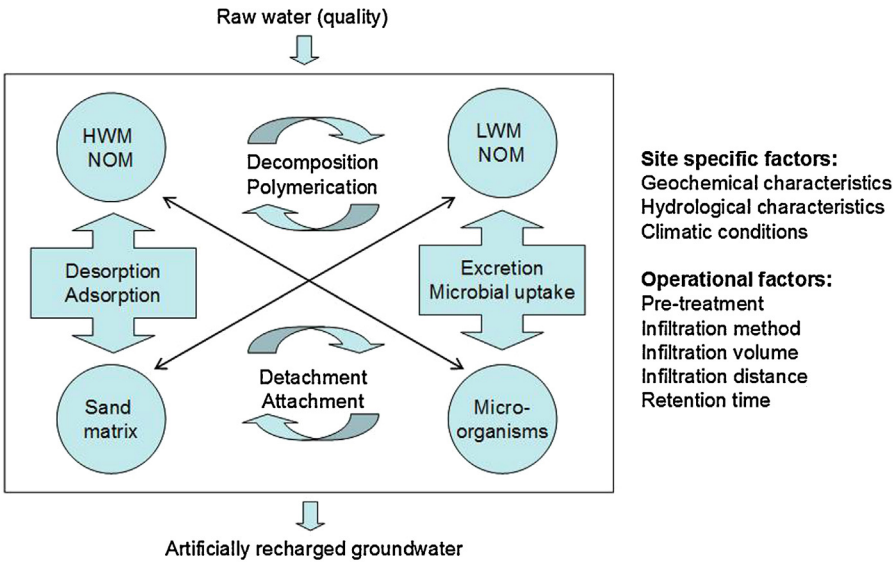

Fig. 13. Transformation of natural organic matter (NOM) and the factors affecting the process in an artificial groundwater recharge aquifer. HMW – high molecular weight, LMW – low molecular weight.
Source: Adapted from Kolehmainen (2008).

Table 9
Trigger criteria for Pawsey Centre groundwater cooling system monitoring.

Analyte	Methods	Reporting	Frequency	Trigger A[c]	Trigger B[d]
Physical					
Water level	Sonde	Online/real time	Continuous[b]	>−5 m production/>−2 m monitoring bores	>−10 m production/>5 m injection bores
Temperature				>10 °C injection/>2 °C monitoring bores	>12 °C injection/>4 °C injection bores
Flow rate/pressure				Minimum operational specifications	Minimum operational specifications
Turbidity				>10 NTU	>20 NTU
Geochemical					
pH	Sonde	Online/real time	Continuous[b]	±1 pH unit within 1 h	±2 pH units within 24 h
Dissolved oxygen				±1 mg L^{-1} DO within 1 h	±2 mg L^{-1} DO within 24 h
Redox (Eh)				±100 mV with 1 h	±200 mV with 24 h
Major ions/metals/nutrients	ICP-OES/MS(1) FIA[a]	Upload to database	6 monthly/as required	Based on pH/DO/Eh/T/NTU	Based on pH/DO/Eh/T/NTU
Biological					
Microbial biomass	Cell counting by microscopy/flow cytometry	Upload to database	6 monthly/as required	10^2–10^3 change over baseline	>10^3 change over baseline
Microbial species	DNA extraction and sequencing			>25% change in composition over baseline	>50% change in composition over baseline
Stygofauna	Field sampling			Variation from baseline	Variation from baseline

[a] Inductively coupled plasma optical emission spectrometry/flow injection analysis.
[b] Reported to accessible database.
[c] Exceedence in shallow or deep bores triggers sampling and analysis of major ions, metals, nutrients, or closer analysis/modification of production/re-injection rates or split between.
[d] Groundwater cooling system shutdown/cooling towers only.

These critical aspects that may affect the operational integrity of groundwater cooling or other geothermal systems have also been considered in detail by Bonte (2013).

The monitoring protocol developed here is primarily based on real time data harvesting and assimilation from 15 in situ multi-parameter sondes measuring pH, Eh, electrical conductivity, dissolved oxygen, turbidity and temperature at (at least) hourly intervals within monitoring, production and injection bores and within the sealed groundwater cooling/heat exchange system in addition to real time flow and pressure in the latter groundwater levels are also monitored in real time in all of the bores and water samples are periodically collected for determining microbial biomass. A central monitoring station is used to aggregate data feeds for subsequent analysis and reporting.

Two operational trigger criteria for the groundwater cooling system have been defined (Table 9) to assist in identifying both moderate and substantial system perturbations requiring further investigation or shutdown, respectively, and transfer of cooling demand to backup cooling towers:

Trigger A (requiring detailed investigation and close monitoring): exceedence of one or more physical, geochemical or biological parameters (Table 9) will trigger water quality sampling (major ions, metals, and nutrients, microbial biomass and microbial species), with results to be referenced to baseline regional and previous operational results. A management team is tasked to assess results as they become available.

Trigger B (immediate shutdown and investigation): exceedence of one or more physical, geochemical or biological parameters (Table 9) will initiate an immediate shutdown of the groundwater cooling system and transfer of cooling requirements to the cooling towers. A management team is tasked to meet to assess results as they become available and to advise on start-up arrangements in line with any regulatory requirements.

6. Conclusions

A rapid assessment protocol has been developed and applied to assess the potential suitability of the Mullaloo aquifer to receive heated water generated from the Pawsey Supercomputer. A multidisciplinary study encompassing a geochemical analysis of the aquifer sediment and microbiological and organic contaminant surveys together with geochemical modelling of the aquifer solute geochemistry has yielded the following information:

Sediment mineralogy and petrography – The Mullaloo aquifer sediments constitute a mature, moderately well sorted, quartz-dominated, possibly shallow marine unit. Minor discrete carbonate and organic matter occurs in the uppermost stratigraphy. In addition, minor heavy minerals dominated by ilmenite occur throughout the stratigraphy, and pyrite is present at depth. In contrast to previous studies, no glauconite was identified.

Sediment geochemistry – Aquifer sediments are quartz-dominated, however, significant amounts of calcite and some pyrite is present in the shallowest and deepest samples, respectively. Concentrations of trace elements are generally low, however, there are significant enrichments of Cr, that is likely to occur within ilmenite or other heavy minerals present within the aquifer. Significant As is also present, principally associated with pyrite within the deep aquifer.

Groundwater geochemistry – The groundwater geochemistry is of a Na-Cl type with neutral to moderately alkaline pH, intermediate redox potential (Eh/pe), and low ionic strength with TDS < 400 mg L^{-1}. Trace element abundances are low and are likely to remain stable under prevailing conditions. Aquifer water quality meets ANZECC drinking water quality guidelines. No BTEX or petroleum hydrocarbons were detected.

Microbiology – Microbial cell counts varied from 1.4×10^5 to 5.2×10^5 cells mL^{-1} (Table 1) with abundances highest in the deepest sample and lowest in the shallowest sample. The cell counts were in the same range as observed by epifluorescence microscopy for the groundwater in a range of local and international locations corresponding to oligotrophic conditions. Dissolved organic carbon, nitrogen and phosphorus are present in the groundwater, which may promote population growth in the presence of electron acceptors. According to the TOC-based guidelines and the observed DOC results for Mullaloo Aquifer, the water quality in the deepest samples indicate slight tendency for bioclogging, where as the shallowest samples indicate notable or strong tendency for bioclogging. As long as electron acceptors are prevented from entering the system, it is likely that microbial numbers will not significantly change, although abundances of the various microbial species comprising the community may vary. Additional sampling and analysis would be required to predict such changes at the species level.

Geochemical modelling – Geochemical modelling indicates there are few, if any adverse implications of increased temperatures on the geochemistry of the Mullaloo aquifer, assuming the reinjected water does not introduce external reagents (e.g. oxygen). If temperature increases are limited to ca. 10 °C as proposed, it is unlikely that any material change to aquifer geochemistry will occur.

Recommendations – Based on the information obtained in this study three recommendations can be made for heat rejection operations at the Pawsey site:

(i) The presence of pyrite within the deeper aquifer in particular signifies the potential for oxidation, acid generation and release of As and potentially other metal/metalloid contaminants. Thus, it is recommended that a closed loop configuration be utilised such that anthropogenic oxygen is not introduced into the Mullaloo aquifer. In addition, it is recommended that withdrawal and return of water be confined to a zone sufficiently above pyrite-bearing stratigraphy if ingress of anthropogenic oxygen occurs during abstraction or re-injection.
(ii) Additional analysis of aquifer sediments be undertaken to confirm the absence of pyrite-bearing stratigraphy prior to operation of any wells.
(iii) Groundwater sampling and analysis should occur monthly during the first year of operation, and at appropriate intervals thereafter, to monitor changes, if any, in groundwater geochemistry and microbiology.

The rapid assessment protocol developed for this study is specific to gaining an environmental baseline prior to impacts of geothermic operations in a shallow aquifer and to make predictions of potential impacts resulting from geothermic operations. In general, due to subsurface geochemical and hydraulic heterogeneity and data scarcity, it is unlikely that all potential impacts can be identified and properly characterised before operations commence. It is always prudent to check performance predictions against actual operation. Therefore upon commissioning of the heat rejection operations it is advisable that a comprehensive aquifer monitoring and sampling schedule be established and run simultaneously with operations along with a monitoring protocol with trigger criteria that facilitate sampling and analysis as supporting evidence for possible modification or shutdown of system operation. The data thus gained would then support assessment of performance of the heat rejection system, regular compliance reporting of the system to regulators and stakeholders, and early identification of any unexpected changes in aquifer status or geochemical state.

Acknowledgements

This work was supported by the Sustainable Energy for the Square Kilometre Array (SESKA) Project. The assistance of Rockwater Pty Ltd in making available drill cutting sediments from MB04 is gratefully acknowledged. Two anonymous reviewers provided excellent comments on this manuscript.

References

Aargard, P., Helgeson, H.C., 1982. Thermodynamic and kinetic constraints on reaction rates among minerals and aqueous solutions. I. Theoretical considerations. Am. J. Sci. 282, 237–285.
Anand, R.R., Paine, M., 2002. Regolith geology of the Yilgarn Craton, Western Australia: implications for exploration. Aust. J. Earth Sci. 49, 3–162.
ANZECC, 2000. Australian and New Zealand Guidelines for Fresh and Marine Water Quality 2000. http://www.mincos.gov.au/publications/australian_and_new_zealand_guidelines_for_fresh_nnd_marine_water_quality
Appleyard, S.J., Angeloni, J., Watkins, R., 2006. Arsenic-rich groundwater in an urban area experiencing drought and increasing population density, Perth, Australia. Appl. Geochem. 21, 83–97.
Banks, D., 2009. Thermogeological assessment of open-loop well-doublet schemes: a review and synthesis of analytical approaches. Hydrogeol. J. 17, 1149–1155.
Bastian, L.V., 1996. Residual soil mineralogy and dune subdivision, Swan Coastal Plain, Western Australia. Aust. J. Earth Sci. 43, 31–44.
Bennett, D., Donnelly, P., Tille, P., 2007. Assessment of the impact of intensification of grazing agriculture on nitrogen and phosphorus levels in the shallow aquifers of the Southern Perth Basin. Dept. Agricult. Food Res. Mgmt., Tech. Rpt., pp. 323.
Bethke, C.M., 2004. The Geochemists Workbench. Release 5.0.
Bonte, M., Stuyfzand, P.J., Hulsmann, A., Van Beelen, P., 2011. Underground thermal energy storage: environmental risks and policy developments in the Netherlands and the EU. Ecol. Soc. 1, 22.
Bonte, M., Stuyfzand, P.J., Van Den Berg, G., 2010. The effects of aquifer thermal energy storage on groundwater quality and the consequences for drinking water production: a case study from the Netherlands. Water Sci. Technol. 63, 1922–1931.
Bonte, M., (PhD Thesis) 2013. Impacts of shallow geothermal energy on groundwater quality. KWR Watercycle Research Institute and VU University Amsterdam, pp. 175.
Brady, P.V., Walther, J.V., 1990. Kinetics of quartz dissolution at low temperatures. Chem. Geol. 82, 253–264.
Brielmann, H., Griebler, C., Schmidt, S.I., Michel, R., Lueders, T., 2009. Effects of thermal energy discharge on shallow groundwater ecosystems. FEMS Microbiol. Ecol. 68, 273–286.
Brielmann, H., Lueders, T., Schreglmann, K., Ferraro, F., Avramov, M., Hammerl, V., Blum, P., Bayer, P., Griebler, C., 2011. Oberflächennahe Geothermie und ihre potenziellen Auswirkungen auf Grundwasserökosysteme. Grundwasser, 1–15.
Brons, H.J., Griffioen, J., Appelo, C.A.J., Zehnder, A.J.B., 1991. (Bio)geochemical reactions in aquifer material from a thermal energy storage site. Water Res. 25, 729–736.
Chopra, P.N., Holgate, F., 2007. Geothermal Energy Potential in Selected Areas of Western Australia: A Consultancy Report by Earthinsite.com Pty Ltd for Geological Survey of Western Australia. Geol. Surv. West. Aust., Statutory Petroleum Exploration Report, G31888 A1 (unpublished).
Collins, L.B., Baxter, J.L., 1984. Heavy mineral-bearing strandline deposits associated with high-energy beach environments, southern Perth Basin, Western Australia. Aust. J. Earth Sci. 31, 287–292.
Cornelius, M., Robertson, I.D.M., Cornelius, A.J., Morris, P.A., 2008. Geochemical mapping of the deeply weathered western Yilgarn Craton of Western Australia, using laterite geochemistry. Geochem. Explor. Environ. Anal. 8, 241–254.
Davidson, W.A., 1995. Hydrogeology and groundwater resources of the Perth Region, Western Australia. West. Aust. Geol. Surv. Bull., 142.
Davidson, W.A., Yu, X., 2006. Perth Regional Aquifer Modelling System PRAMS Model Development: Hydrogeology and Groundwater Modelling. Dept. Water, Hydrogeological Record Series HG 20.
Descourvieres, C., Douglas, G., Leyland, L., Hartog, N., Prommer, H., 2011. Compositional variation and chemical provenance signature of post-rift passive margin sediments of the early Cretaceous Leederville Formation in the Perth Basin, Western Australia. Sediment. Geol. 226, 62–76.
Douglas, G.B., Patterson, B.M., Davis, G.B., Wendling, L.A., Coleman, S., Furness, A.J., 2008. Assessment of Acid Sulfate Soils and Surface Water and Groundwater Quality at Baigup Reserve, Western Australia. CSIRO Water for a Healthy Country Flagship Report, August 2008, 51 pp.
Dincer, I., 2002. Thermal energy storage systems as a key technology in energy conservation. Int. J. Energy Res. 26, 567–588.
Farnleitner, A.H., Wilhartitz, I., Ryzinska, G., Kirschner, A.K.T., Stadler, H., Burtscher, M.M., Hornek, R., Szewzyk, U., Herndl, G., Mach, R.L., 2005. Bacterial dynamics in spring water of alpine karst aquifers indicates the presence of stable autochthonous microbial endokarst communities. Environ. Microbiol. 7, 1248–1259.
Ferguson, G., 2007. Heterogeneity and thermal modelling of ground water. Groundwater 45, 485–490.

Ferguson, G., Woodbury, A.D., 2006. Observed thermal pollution and post-development simulations of low-temperature geothermal systems in Winnipeg, Canada. Hydrogeol. J. 14, 1206–1215.
Ghori, K.A.R., 2008. The search for Western Australia's geothermal resources. Geol. Surv. West. Aust. Ann. Rev., 25–31, 2006-07.
Gozzard, J.R., 2007. Geology and landforms of the Perth Region. West. Aust. Geol. Surv., 126.
Griffioen, J., Appelo, C.A.J., 1993. Nature and extent of carbonate precipitation during aquifer thermal energy storage. Appl. Geochem. 8, 161–176.
Gringarten, A.C., Sauty, J.P., 1975. Theoretical study of heat extraction from aquifers with uniform regional flow. J. Geophys. Res. 80, 4956–4962.
Groves, D.I., Barrett, F.M., Binns, R.A., McQueen, K.G., 1977. Spinel phases associated with metamorphosed volcanic-type iron-nickel sulfide ores from Western Australia. Econ. Geol. 72, 1224–1244.
Hoefel, D., Grooby, W.L., Monis, P.T., Andrews, S., Saint, C.P., 2003. Enumeration of water-borne bacteria using viability assays and flow cytometry: a comparison to culture-based techniques. J. Microbiol. Methods 55, 585–597.
Holm, T.R., 1986. Groundwater geochemistry of aquifer thermal-energy storage. Abstr. Pap. Am. Chem. Soc. 192 (77-GEOC).
Horne, R.N., 1982. Geothermal reinjection experience in Japan. J. Petrol. Technol. 34, 495–503.
iVEC, 2010. The Pawsey Centre. http://www.ivec.org/sites/default/files/PAWSEY%20INFO%20SHEET%20SEPT2010.pdf
Kim, J., Lee, Y., Yoon, W.S., Jeon, J.S., Koo, M.-H., Keehm, Y., 2010. Numerical modelling of aquifer thermal energy storage system. Energy 35, 4955–4965.
Kimura, H., Sugihara, M., Yamamoto, H., Patel, B.K.C., Kato, K., Hanada, S., 2005. Microbial community in a geothermal aquifer associated with the subsurface of the Great Artesian Basin, Australia. Extremophiles 9, 407–414.
King, L.K., Parker, B.C., 1988. A simple, rapid method for enumerating total viable and metabolically active bacteria in groundwater. Appl. Environ. Microbiol. 54, 1630–1631.
Kolehmainen, R., (Thesis for the Degree of Doctor of Technology) 2008. Natural Organic Matter Biodegradation and Microbial Community Dynamics in Artificial Groundwater Recharge. Tampere Univ. Technol., Tampere, Finland, pp. 11.
Kuhn, M., Bartels, J., Iffland, J., 2002. Predicting reservoir property trends under heat exploitation: interaction between flow, heat transfer, transport, and chemical reactions in a deep aquifer at Strausland, Germany. Geothermics 31, 725–749.
Li, S., Liu, S., Shang, Y., Du, G., 2011. Numerical study of distribution characteristics and influencing factors on geo-temperature field of groundwater heat pump. Adv. Mater. Res. 320, 536–541.
Norrish, K., Chappell, B.W., 1977. X-ray fluorescence spectrometry. In: Zussman, J. (Ed.), Physical Methods in Determinative Mineralogy. Academic Press, London, pp. 201–272.
O'Shaughnessy, P.T., 1973. Determination of trace levels of chromium in ilmenite by atomic absorption spectrometry. Anal. Chem. 45, 1946–1947.
Panichi, C., 2004. Geochemical impact of re-injecting geothermal waste waters; example, Larderello, Italy in Energy, waste and the environment; a geochemical perspective. Geol. Soc. Spec. Publ. 236, 337–354.
Papadopulos, S.S., Larson, S.P., 1978. Aquifer storage of heated water: Part II. Numerical simulation of field results. Groundwater 16, 242–248.
Pérez-Paricio, A., (PhD Thesis) 2000. Integrated Modelling of Clogging Processes in Artificial Groundwater Recharge. Department of Geotechnical Engineering & GeoSciences Tech. Univ., Catalonia UCP, Barcelona, Spain.
Perlinger, J.A., Almendinger, J.E., Urban, N.R., Eisenreich, S.J., 1987. Groundwater geochemistry of aquifer thermal-energy storage – long-term test cycle. Water Resour. Res. 23, 2215–2226.
Post, V.E.A., 2011. PHREEQC for Windows Version 2.18.00. A Hydrogeochemical Transport Model by D.L. Parkhurst and C.A.J. Appelo. Graphical User Interface by V.E.A. Post. http://pfw.antipodes.nl/index.html
Quilty, P.G., 1974. Cainozoic stratigraphy in the Perth area. West. Aust. R. Soc. J. 57, 16–31.
Regenauer-Lieb, K., Horowitz, F., 2007. The Perth Basin geothermal opportunity: September 2007 Petroleum in Western Australia, Western Australia's Digest of Petroleum Exploration, Development and Production. Dept. Indust. Resour., Perth, pp. 42–44.
Robertson, W.J., Franzmann, P.D., Mee, B.J., 2000. Spore-forming, desulfosporosinus-like sulfate-reducing bacteria from a shallow aquifer contaminated with gasoline. J. Appl. Microbiol. 88, 248–259.
Robertson, W.J., Franzmann, P.D., Mee, B.J., 2001. *Desulfosporosinus meridiei* sp. nov., a spore-forming sulfate-reducing bacterium isolated from gasoline-contaminated groundwater. Int. J. Syst. Evol. Microbiol. 51, 133–140.
Rockwater Pty Ltd, (Unpublish. Rpt. for CSIRO) 2011a. Aquifer Heat Rejection for Cooling the Proposed Pawsey Centre. H2 Level Hydrogeological Assessment.
Rockwater Pty Ltd, (Unpublish. Rpt. for CSIRO) 2011b. Bore Completion and Test Pumping Report.
Rockwater Pty Ltd, (Unpublish. Rpt. for CSIRO) 2011c. Preliminary H3 Level Hydrogelological Assessment for Groundwater Supply and Injection for the Proposed Pawsey Supercomputer.
Sarukkalige, P.R., 2011. Assessment of spatial variation of groundwater quality and its relationship with land use in metropolitan Perth. J. Water Resour. Protect. 3, 311–317.
Shimizu, S., Akiyama, M., Naganuma, T., Fujioka, M., Nako, M., Ishijima, Y., 2007. Molecular characterization of microbial communities in deep coal seam groundwater of northern Japan. Geobiology 5, 423–433.
Simpson III, E.S., 1912. Notes on laterite in Western Australia. Geol. Mag. (Decade V) 9, 399–406.
Snap Sampler, 2011. ProHydro, Inc., USA, www.snapsampler.com
Tawney, R., Khan, Z., Zachary, J., 2005. Economic and performance evaluation of heat sink options in combined cycle applications. J. Eng. Gas Turbines Power 127, 397–403.
Taylor, S.R., McLennan, S.M., 1985. The Continental Crust: Its Composition and Evolution. Blackwell, Oxford, pp. 312.
Wilhartitz, I., Mach, R.L., Teira, E., Reinthaler, T., Herndl, G.J., Farnleitner, A.H., 2007. Prokaryotic community analysis with CARD-FISH in comparison to FISH in ultra-oligotrophic ground- and drinking water. J. Appl. Microbiol. 103, 871–881.
Winters, A.L., 1992. Summary of Research on Microbiological Processes. International Energy Agency Subtask D Final Report 64. Dept. Biol. Sci. Univ. of Alabama.
Yesertener, C., 2010. Hydrogeochemical Assessment of the Superficial Aquifer. Perth Metropolitan Area. Dept. Water Hydrogeological Rec. Ser. Rpt. No HG37, August 2010, 174 pp.
Yu, Z., Zhang, Y., Wang, C., 2011. Hydro-thermal coupled numerical simulation for groundwater storage energy and its application. In: Intl. Conf. Electric Technology and Civil Engineering ICETCE, April 22–24, 2011, Lushan, China, pp. 3202–3206 http://www.icetce.org

Glossary

Megawatt thermal: 10^6 watts of thermal power
Petrographic analysis: microscopic analysis of rock thin sections
Flow cytometry: is a technique for counting and examining microscopic particles, such as cells, by suspending them in a stream of fluid and passing them by an electronic detection apparatus.
DAPI or 4′,6-diamidino-2-phenylindole: is a fluorescent stain that binds strongly to DNA in both live and dead cells and which is used extensively in fluorescence microscopy.
Epifluorescence microscopy: is a method of fluorescence where excitatory light is passed from above, through the objective and then onto the specimen instead of passing it first through the specimen.
Ultraoligotrophic: extremely low concentrations of plant nutrients, nitrogen and phosphorus